

Identification of the Gene Cluster for the Anaerobic Degradation of 3,5-Dihydroxybenzoate (α -Resorcyate) in *Thauera aromatica* Strain AR-1

Águeda Molina-Fuentes,^a Daniel Pacheco,^a Patricia Marín,^a Bodo Philipp,^{b,c} Bernhard Schink,^c Silvia Marqués^a

Consejo Superior de Investigaciones Científicas, Estación Experimental del Zaidín, Department of Environmental Protection, Granada, Spain^a; Westfälische Wilhelms-Universität Münster, Institut für Molekulare Mikrobiologie und Biotechnologie, Münster, Germany^b; University of Konstanz, Department of Biology, Constance, Germany^c

Thauera aromatica strain AR-1 degrades 3,5-dihydroxybenzoate (3,5-DHB) with nitrate as an electron acceptor. Previous biochemical studies have shown that this strain converts 3,5-DHB to hydroxyhydroquinone (1,2,4-trihydroxybenzene) through water-dependent hydroxylation of the aromatic ring and subsequent decarboxylation, and they suggest a pathway homologous to that described for the anaerobic degradation of 1,3-dihydroxybenzene (resorcinol) by *Azoarcus anaerobius*. Southern hybridization of a *T. aromatica* strain AR-1 gene library identified a 25-kb chromosome region based on its homology with *A. anaerobius* main pathway genes. Sequence analysis defined 20 open reading frames. Knockout mutations of the most relevant genes in the pathway were generated by reverse genetics. Physiological and biochemical analyses identified the genes for the three main steps in the pathway which were homologous to those described in *A. anaerobius* and suggested the function of several auxiliary genes possibly involved in enzyme maturation and intermediate stabilization. However, *T. aromatica* strain AR-1 had an additional enzyme to metabolize hydroxyhydroquinone, a putative cytoplasmic quinone oxidoreductase. In addition, a specific tripartite ATP-independent periplasmic (TRAP) transport system was required for efficient growth on 3,5-DHB. Reverse transcription-PCR (RT-PCR) analysis showed that the pathway genes were organized in five 3,5-DHB-inducible operons, three of which have been shown to be under the control of a single LysR-type transcriptional regulator, DbdR. Despite sequence homology, the genetic organizations of the clusters in *T. aromatica* strain AR-1 and *A. anaerobius* differed substantially.

Aromatic compounds are ubiquitous substrates for bacteria in natural habitats. Pathways of aerobic microbial degradation of aromatics have been studied in detail, but our knowledge on anaerobic degradation pathways is comparatively scarce, and the diversity of pathways is certainly underestimated. Anaerobic degradation differs substantially from aerobic degradation, as the well-known O₂-dependent oxygenase reactions cannot be applied in the absence of molecular oxygen. In general, anaerobic degradation attacks the aromatic ring by a reduction reaction to overcome its mesomery-enhanced stability (1, 2). The most common central intermediate formed by bacteria in the absence of oxygen is benzoyl coenzyme A (benzoyl-CoA). Numerous compounds, such as toluene, benzoate, phenol, cresols, and phenylacetate, among others, are transformed through different peripheral pathways to this central intermediate (3). Benzoyl-CoA is reductively dearomatized to render 1,5-dienoyl-CoA, which undergoes further reduction and ring opening through a series of reactions similar to β -oxidation (4). Di- and trihydroxylated aromatic compounds such as resorcinol (1,3-dihydroxybenzene), phloroglucinol (1,3,5-trihydroxybenzene), or hydroxyhydroquinone (1,2,4-trihydroxybenzene) can be dearomatized in fermenting and sulfate-reducing bacteria by reductive reactions directly without channeling reactions (1, 2, 5).

In contrast, two denitrifying bacteria use an entirely different degradation strategy for the anaerobic degradation of dihydroxylated aromatics. The obligately denitrifying betaproteobacterium *Azoarcus anaerobius* attacks resorcinol by an oxidative rather than a reductive reaction and hydroxylates the aromatic ring at position 4 by using a resorcinol hydroxylase to form hydroxyhydroquinone (HHQ) (6) (Fig. 1). Hydroxylation of resorcinol can be detected *in vitro* in the membrane fraction of *A. anaerobius* with

K₃Fe(CN)₆ as an electron acceptor (6–8). In the second step, hydroxyhydroquinone is oxidized to 2-hydroxy-1,4-benzoquinone (HBQ). Further metabolism of 2-hydroxy-1,4-benzoquinone to malate and acetate proceeds via so-far-unknown reactions (Fig. 1).

A similar pathway was described for the degradation of 3,5-dihydroxybenzoate (3,5-DHB) (α -resorcyate) in the denitrifying betaproteobacterium *Thauera aromatica* strain AR-1. This strain also uses a water-dependent oxidative reaction to convert 3,5-DHB to hydroxyhydroquinone in two steps: the aromatic ring is hydroxylated at position 2, yielding 2,3,5-trihydroxybenzoate, which is decarboxylated to hydroxyhydroquinone in a reaction that is stimulated in the presence of an unidentified cytoplasmic factor (9) (Fig. 1). The initial 3,5-DHB-hydroxylating activity is membrane associated, and a membrane-bound hydroxyhydroquinone dehydrogenase activity was also found in cell extracts of 3,5-DHB-induced cultures (10). This suggests that the anaerobic

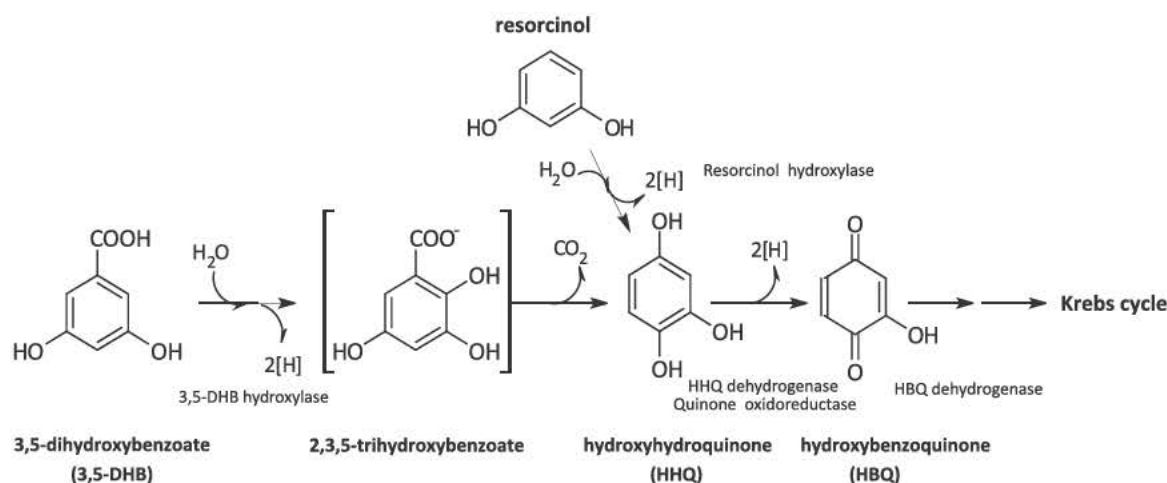


FIG 1 The *T. aromatica* strain AR-1 3,5-DHB degradation pathway and the *A. anaerobius* resorcinol degradation pathway converge in the central intermediate hydroxyhydroquinone.

3,5-DHB degradation pathway of *T. aromatica* strain AR-1 parallels *A. anaerobius* resorcinol degradation, with hydroxyhydroquinone as the common central intermediate (Fig. 1). To our knowledge, these two bacteria are so far the only ones known to use this oxidative pathway to degrade an aromatic compound in the absence of oxygen.

This unexplored metabolic pathway was first accessed at the genetic level by heterologous expression of an *A. anaerobius* cosmid library in *T. aromatica* strains (7), which allowed the identification of a cosmid encompassing the gene cluster for resorcinol degradation. Mutational analysis identified the genes for the two first reactions in resorcinol degradation, *rehLS* for the resorcinol hydroxylase and *btdLS* for the hydroxyhydroquinone dehydrogenase, and the genes coding for an enzyme system initiating the further degradation of the product hydroxybenzoquinone, *bqdLMS* (7).

It is so far not possible to grow *A. anaerobius* on agar surfaces, impeding a more detailed genetic analysis of the pathway. In contrast, we have been able to adapt and apply genetic tools to the manipulation of *T. aromatica* strain AR-1, providing the possibility to use the 3,5-DHB degradation pathway in this strain as model to further characterize this conserved oxidative pathway. On the other hand, the regulation of these pathways is completely unknown at the molecular level. The main enzymes of the pathway are induced by the presence of the substrate, although in *T. aromatica*, the 3,5-DHB degradation pathway is also subject to catabolite repression by benzoate (10). The second goal of this study was to identify regulators for 3,5-DHB degradation in *T. aromatica* strain AR-1.

We initially identified the gene cluster for the pathway based on sequence similarity to key genes of the resorcinol degradation cluster in *A. anaerobius*, and we characterized mutants with insertion mutations in relevant genes. With the present study, we have gained access to elucidating at the genetic level this anaerobic pathway which uses oxidative reactions to overcome the aromatic structure, thus increasing our knowledge of the diversity of the microbial metabolism of aromatic compounds.

MATERIALS AND METHODS

Bacterial strains, plasmids, and culture conditions. The bacterial strains and plasmids used in this work are summarized in Table 1. *Thauera* aro-

matica strain AR-1 and its mutant derivatives and transconjugants were cultured anaerobically at 30°C without shaking in 50- or 100-ml infusion bottles containing nonreduced Widdel mineral medium under nitrogen gas (6). The medium was buffered with 30 mM 3-(*N*-morpholino)propanesulfonic acid (MOPS) instead of bicarbonate and supplemented with 8 mM potassium nitrate. Carbon sources stored in sterile infusion bottles under nitrogen gas were added to the cultures with syringes to the specified final concentrations. For all genetic manipulations, *T. aromatica* strain AR-1 and derivatives were grown aerobically in Widdel mineral medium supplemented with 5 mM succinate or glutarate as the carbon source. Solid media were prepared with 1.6% twice-washed Difco agar. *Escherichia coli* strains HB101, DH5 α , and CC118 λ *pir* were grown aerobically at 37°C in Luria-Bertani (LB) medium. When appropriate, antibiotics were used at the following concentration: tetracycline, 10 μ g ml⁻¹; chloramphenicol, 30 μ g ml⁻¹; ampicillin, 100 μ g ml⁻¹; kanamycin, 50 μ g ml⁻¹; streptomycin, 50 μ g ml⁻¹, and gentamicin, 10 μ g ml⁻¹ (except for *T. aromatica*, for which tetracycline and kanamycin were used at 5 μ g ml⁻¹ and 25 μ g ml⁻¹, respectively).

Growth experiments. To analyze 3,5-DHB degradation and nitrate reduction by *T. aromatica* strain AR-1 and mutant derivatives, 100-ml serum bottles containing 75 ml of anaerobic Widdel mineral medium supplemented with the required antibiotics and 3,5-DHB (1 mM) and/or succinate (2 mM) were inoculated with 1% of the exponentially growing wild-type and mutant *T. aromatica* strain AR-1 cultures and incubated at 30°C. Samples were taken anoxically with a sterile syringe flushed with N₂ at the designated time points and used immediately for determination of optical density at 600 nm (OD₆₀₀) in a Shimadzu UV-266 spectrophotometer.

Construction and screening of a genome library of *Thauera aromatica* strain AR-1. Preparation of plasmids and chromosomal DNA, digestion with restriction endonucleases, ligation, agarose gel electrophoresis, and Southern blotting were performed using standard methods (11). To prepare a genome library of *Thauera aromatica* strain AR-1, 11 μ g of genomic DNA from the strain was partially digested with PstI, and 20- to 30-kb fragments were ligated to a PstI-digested and dephosphorylated pLAFR3 vector. Gigapack III XL packaging extract (Stratagene) was used to package the recombinant DNA. The phage particles obtained were transfected into *E. coli* HB101, and colonies were grown on LB agar plates with tetracycline. The colonies harvested and pooled in LB liquid medium constituted the gene library. Screening of approximately 3,400 clones of the library was carried out by colony hybridization with randomly digoxigenin (DIG)-labeled probes obtained by PCR amplification of internal fragments of the *A. anaerobius* *orf14*, *rehL*, and *bqdL* genes with specific primers using a DIG-DNA labeling kit (Roche). Twenty cosmids hybridizing with at least one of the probes were initially selected, and finally a

TABLE 1 Bacterial strains and plasmids used in this work

Strain, plasmid, or cosmid	Genotype or relevant characteristics	Reference
Strains		
<i>Escherichia coli</i>		
HB101	<i>supE44 hsdS20</i> ($r_B^- m_B^-$) <i>recA13 ara-14 proA2 lacY1 galK2 rpsL20</i> (Sm^r) <i>xyl-5 mtl-1</i>	35
CC118	Δ (<i>ara-leu</i>) <i>araD</i> Δ <i>lacX74 galE galK phoA20 thi-1 rpsE</i> (Sp^r) <i>rpoB</i> (Ri^r) <i>argE recA1</i>	36
CC118 λ pir	CC118 lysogenized with λ pir	37
DH5 α	<i>endA1 hsdR17 supE44 thi-1 recA1 gyrA</i> (Nal^r) <i>relA1</i> Δ (<i>argF-lac</i>)U169 <i>depR</i> (ϕ 80 <i>dlac</i> Δ (<i>lacZ</i>)M15)	11
<i>Pseudomonas putida</i> KT2440		
<i>Thauera aromatica</i>		
AR-1	Wild-type strain, degrades 3,5-DHB under denitrifying conditions (DSM-11528)	39
AR-1 <i>orf3</i>	Km^r , <i>T. aromatica</i> AR-1 mutant bearing pPM <i>orf3</i> plasmid integrated in the chromosome	This work
AR-1 <i>korAB</i>	Gm^r , <i>T. aromatica</i> AR-1 mutant, <i>korAB</i> genes partially deleted and replaced by a gentamicin resistance cassette	This work
AR-1 <i>dbhL</i>	Km^r , <i>T. aromatica</i> AR-1 mutant bearing pAM <i>dbhL</i> plasmid integrated in the chromosome	This work
AR-1 <i>dbhS</i>	Km^r , <i>T. aromatica</i> AR-1 mutant bearing plasmid pAM <i>dbhS</i> integrated in the chromosome.	This work
AR-1 <i>dctP</i>	Km^r , <i>T. aromatica</i> AR-1 mutant bearing plasmid pAM <i>orf13</i> integrated in the chromosome.	This work
AR-1 <i>btdL</i>	Gm^r , <i>T. aromatica</i> AR-1 mutant, <i>btdL</i> gene disrupted by a gentamicin resistance cassette	This work
AR-1 <i>orf17</i>	Km^r , <i>T. aromatica</i> AR-1 mutant bearing plasmid pPM <i>orf17</i> integrated in the chromosome	This work
AR-1 <i>orf18</i>	Km^r , <i>T. aromatica</i> AR-1 mutant bearing plasmid pAM <i>orf18</i> integrated in the chromosome	This work
AR-1 <i>bqdM</i>	Km^r , <i>T. aromatica</i> AR-1 mutant bearing plasmid pAM <i>bqdM</i> integrated in the chromosome	This work
AR-1 <i>orf20</i>	Km^r , <i>T. aromatica</i> AR-1 mutant bearing plasmid pAM <i>orf20</i> integrated in the chromosome	This work
AR-1 <i>orf21</i>	Km^r , <i>T. aromatica</i> AR-1 mutant bearing plasmid pAM <i>orf21</i> integrated in the chromosome	This work
AR-1 <i>bqdL</i>	Km^r , <i>T. aromatica</i> AR-1 mutant bearing plasmid pAM <i>bqdL</i> integrated in the chromosome	This work
AR-1 <i>dbdR</i>	Km^r , <i>T. aromatica</i> AR-1 mutant bearing plasmid pPM <i>dbdR</i> integrated in the chromosome	This work
AR-1 <i>qorA</i>	Gm^r , <i>T. aromatica</i> AR-1 mutant, <i>qorA</i> gene disrupted by a gentamicin resistance cassette	This work
AR-1 <i>orf27</i>	Km^r , <i>T. aromatica</i> AR-1 mutant bearing plasmid pPM <i>orf27</i> integrated in the chromosome	This work
AR-1 <i>btdL qorA</i>	Km^r , <i>T. aromatica</i> AR-1 <i>qorA</i> derivative bearing an internal deletion in the <i>btdL</i> gene	This work
Plasmids		
pCHESIOKm	Ap^r , Km^r , pUC18 bearing RP4 <i>oriT</i> and the Ω interposon from pHP45 Ω Km as HindIII fragment.	12
pKNG101	Sm^r , Sac^s , RK2 <i>oriV</i>	40
pRK600	Cm^r , ColE1 <i>oriV</i> , RK2 <i>mob</i> ⁺ <i>tra</i> ⁺	41
pJB3Tc19	Broad-host range IncP1 cloning vector, Tc^r , Ap^r	16
pPM <i>orf3</i>	Internal fragment of <i>orf3</i> (669 bp) cloned between the KpnI and BamHI sites of pCHESIOKm	This work
pPM <i>korAB</i>	Gentamicin resistance cassette flanked by the upstream sequence of <i>korA</i> (842 bp) and the end sequence of <i>korB</i> and its downstream region (715 bp) cloned in pKNG101	This work
pPM <i>btdL</i>	<i>btdL</i> gene and its flanking region (2,089 bp) interrupted by a Km^r cassette, cloned in pKNG101	This work
pAM <i>dbhL</i>	Internal fragment of <i>dbhL</i> (411 bp) cloned between the SacI and EcoRI sites of pCHESIOKm	This work
pAM <i>dbhS</i>	Internal fragment of <i>dbhS</i> (584 bp) cloned between the SacI and EcoRI sites of pCHESIOKm	This work
pAM <i>orf13</i>	Internal fragment of <i>orf13</i> (650 bp) cloned between the SacI and EcoRI sites of pCHESIOKm	This work
pPM <i>orf17</i>	Internal fragment of <i>orf17</i> (546 bp) cloned between the EcoRI and XbaI sites of pCHESIOKm	This work
pAM <i>orf18</i>	Internal fragment of <i>orf18</i> (819 bp) cloned between the SacI and EcoRI sites of pCHESIOKm	This work
pAM <i>bqdM</i>	Internal fragment of <i>bqdM</i> (738 bp) cloned between the SacI and EcoRI sites of pCHESIOKm	This work
pAM <i>orf20</i>	Internal fragment of <i>orf20</i> (700 bp) cloned between the SacI and EcoRI sites of pCHESIOKm	This work
pAM <i>orf21</i>	Internal fragment of <i>orf21</i> (1,010 bp) cloned between the SacI and EcoRI sites of pCHESIOKm	This work
pAM <i>bqdL</i>	Internal fragment of <i>bqdL</i> (863 bp) cloned between the SacI and EcoRI sites of pCHESIOKm	This work
pPM <i>dbdR</i>	Internal fragment of <i>dbdR</i> (677 bp) cloned between the SacI and BamHI sites of pCHESIOKm	This work
pPM <i>qorA</i>	<i>qorA</i> gene and its flanking regions (780 and 970 bp) interrupted by a gentamicin resistance cassette, cloned in pKNG101	This work
pPM <i>orf27</i>	Internal fragment of <i>orf27</i> (877 bp) cloned in the EcoRI site of pCHESIOKm	This work
pJB-dbhLS	pJB3Tc19 derivative harboring the <i>dbhLS</i> genes under control of the P_{lac} promoter	This work
pJB- <i>orf20</i>	pJB3Tc19 derivative harboring the <i>orf20</i> gene under control of the P_{lac} promoter	This work
pJB- <i>bqdS</i>	pJB3Tc19 derivative harboring the <i>bqdS</i> gene under control of the P_{lac} promoter	This work
pJB- <i>bqdL</i>	pJB3Tc19 derivative harboring the <i>bqdL</i> gene under control of the P_{lac} promoter	This work
Cosmids		
pLAFR3	Tc^r , cos , RK2 <i>oriV</i> , RK2 <i>oriT</i>	42
pCOS4	Tc^r , pLAFR3 containing a 23.6-kb chromosomal fragment from <i>T. aromatica</i> AR-1	This work
pCOS12	Tc^r , pLAFR3 containing a chromosomal fragment from <i>T. aromatica</i> AR-1	This work
pCOS19	Tc^r , pLAFR3 containing a chromosomal fragment from <i>T. aromatica</i> AR-1	This work
pCOS2B	Tc^r , pLAFR3 containing a chromosomal fragment from <i>T. aromatica</i> AR-1	This work
pCOS6B	Tc^r , pLAFR3 containing a chromosomal fragment from <i>T. aromatica</i> AR-1	This work

TABLE 2 Oligonucleotide primers used in this work

Primer pair	Sequences (5' to 3')	Location (product ^a)	Expected size (bp)
rt-korA_3'/rt-korB_5'	AACAGAGCCACGGCGCCAG/CGAACACGTTGGTGTAGGCG	<i>orf5/orf6</i> intergenic region (1)	350
rt-korB_3'/rt-rhL_5'	GAAGGCCAGCGTCCGATCCG/GTGCATCTGCACGGTGAG	<i>orf6/dbhL</i> intergenic region (2)	580
FupK/RdK	CATCTGCGCGACAAGCAG/GTCCGGAGCCGGATCGAG	<i>korAB</i> and flanking regions	3,672
rhLF/rhLR	GACGCAGCGCTCAGCAGC/AACGCCATCGGCACGACC	<i>dbhL</i> internal region	411
rhSF/rhSR	AGAACAGCGGATCGACGGC/GGCCCGGAGGTGGCCGG	<i>dhbS/orf9</i> intergenic region (4)	584
rt-rhL_3'/rt-rhS_5'	CGTCAATCAGCTCAGCCG/GGCCGAGCTTGCCATTTC	<i>dbhL/dhbS</i> intergenic region (3)	277
rt-rhS_3'/rt-cup_5'	TTCGCCATGGAAGTGAAG/GCACGGTCGACGAGCCTTG	<i>dhbS/orf9</i> intergenic region (5)	160
rt-cup_3'/rt-hyp_5'	TCGATCCGCTGTCTACTTC/TGACGTCTAGTCTTGGCCG	<i>orf9/orf10</i> intergenic region (6)	380
rt-hyp_3'/rt-deh_5'	TCCCTCAACGGCAAGGACTAC/TGCCATCGCCAGATGGACG	<i>orf10/btdL</i> intergenic region (7)	448
rt-deh_3'/rt-m24_5'	GATCGCGCAGACCTATG/GGATAGTCGATGCCGAGTTC	<i>btdL/orf12</i> intergenic region (8)	396
orf9F/orf12R	CTGTCTACTTCGAATTCCAGG/TCAGGCACTGGATCTCTCGC	<i>btdL</i> and flanking regions	2,089
rt-m24_3'/rt-dctP_5'	AAGTGGTGGTGACGAAGGAC/CCGTCTCGTATAGATGTG	<i>orf12/dbtP</i> intergenic region (10)	329
m24F/m24R	GGAATCGGCATCGACTATC/TGCTGGCCATCGACCACCTC	<i>orf12</i> internal fragment (9)	450
rt-dctP_3'/rt-smallper_5'	TGCGCAAAGCAGTTCATCGAC/GGCGCCATGAGGACGTAGC	<i>dbtP/dbtQ</i> intergenic region (11)	259
rt-smallper_3'/rt-dctM_5'	CCACCAGGCCGTGCAGTCG/AAGCGGAATGGCGAGGAACC	<i>dbtQ/dbtM</i> intergenic region (12)	236
rt-esr_5'/rt- α hyd_3'	CTTGATGATCTTCTGCGG/TGGTCCGATCGAAGACAGC	<i>orf17/orf16</i> intergenic region (13)	330
rt-mob_3'/rt-bqdhM_5'	ACAACCAGCCGCCCTAC/TCATAGCTGTTGTTGTCG	<i>orf18/bqdM</i> intergenic region (14)	167
rt-bqdhM_3'/rt-suc_5'	AAGCCGAGCTGATCGCCAC/AGGTCCGGATCGGTCAATTC	<i>bqdM/orf20</i> intergenic region (15)	338
rt-suc_3'/rt-p47k_5'	TTCTACACCTGGCAGCTGG/GCAGCACACGCAACCGTTGG	<i>orf20/orf21</i> intergenic region (16)	515
rt-p47k_3'/rt-bqdhL_5'	TCGACATCGAGCAGGACGAT/TCGAGATGGGCGAGGCACCTG	<i>orf21/bqdL</i> intergenic region (17)	495
rt-bqdhL_3'/rt-hypprot_5'	ACAGCGTGGCAAGACCAAC/CCGATCACCTCGACGAAG	<i>bqdL/orf23</i> intergenic region (18)	400
rt-hypprot_3'/rt-pydh_5'	CCAGACCTGGGTCTATTTC/CAGGATCTTGGCCGAGAATGC	<i>orf23/bqdS</i> intergenic region (19)	338
rt-pydh_3'/rt-lysR_5'	TGTGGTTCGATCATCGCGT/TTTCGTCCACCGACTGC	<i>bqdS/dbdR</i> intergenic region (20)	289
lysRR/lysRR2	GCGAAGGTGCTGTTCTGTC/GAACAACCGCTTCGGCACC	<i>dbdR</i> internal region	677
rt-lysR_3'/rt-Zaldehy_5'	GATGCCGGCGTGAACATCG/TCGCGTCTCGGATTGACC	<i>dbdR/qorA</i> intergenic region (21)	430
FupQ/RdQ	CGGGCAATTCGATCTCGG/TGACCAACCTGATTTTCC	<i>qorA</i> and flanking regions	1,814
HindIII dbhLSF/XbaI dbhLSR	AAGCTTGGGCTGGATAGACTGCCAGGCATCG/ TCTAGACGCCACGTGCATCACCAGATTCCACT	<i>dbhL/dbhS</i> coding sequence	3,979
HindIII bqdmF/XbaI bqdmMR	AAGCTTACCCTCGTGCCGCCGCCCTCC/ TCTAGAGCCGGCGCACAGCAATCAGATGTG	<i>bqdm</i> coding sequence	1,492
HindIII bqdlF/XbaI bqdlLR	AAGCTTGCGCAGTGCCCGGCACC/ AAGCTTGCGCAGTGCCCGGCACC	<i>bqdl</i> coding sequence	2,264
HindIII orf20F/XbaI orf20R	AAGCTTCCATTTCCGAAATCTTCCAGGAC/ TCTAGACGCCCTCGCTCATGCCGGAATC	<i>orf20</i> coding sequence	1,552
HindIII orf21/XbaI orf21R	AAGCTTACGTCAAACGCGGTGCC/ TCTAGACGACGCATCGGTTTCGATTC	<i>orf21</i> coding sequence	1,154

^a The numbers in parentheses refer to the PCRs in Fig. 2.

23-kb-insert cosmid (pCOSM4) was shotgun sequenced. Probes against the two ends of this insert were generated as described above and used to select four additional cosmids covering its flanking regions. The four cosmids were pooled and pyrosequenced. Two final contigs could be assembled: one of them (13,363 bp) was homologous to the *Thauera* sp. strain MZ1T chromosome and contained a gene cluster related to nitrate respiration, while the other one (36,128 bp) showed homology with the *Azoarcus anaerobius* resorcinol degradation cluster. No connecting sequence between the two cosmids could be found.

Cosmid sequencing. The selected cosmids from the *T. aromatica* strain AR-1 library were either shotgun sequenced at Macrogen Inc. (Seoul, South Korea) or pyrosequenced using a Roche 454 GSFLX titanium system with 20 \times coverage at GATC-Biotech (Constance, Germany). Small gaps between the resulting contigs were covered using PCR, and controversial PstI sites were checked by sequencing the corresponding PCR-amplified region from *T. aromatica* genomic DNA.

Site-specific homologous inactivation of genes in the *T. aromatica* strain AR-1 3,5-DHB degradation cluster. Mutant strains with inactivated chromosomal versions of *orf3*, *dbhL*, *dhbS*, *orf13*, *orf17*, *orf18*, *bqdM*, *orf20*, *orf21*, *bqdL*, and *orf25* were generated by single homologous recombination using plasmid pCHESI Ω Km, a pUC18-based vector bearing the *oriT* transfer origin of RP4 and the Ω -Km interposon of pHP45 Ω Km (12) (Table 1). To generate the desired mutation, an internal fragment (mini-

um size, 500 bp) of the target gene was amplified by PCR with the appropriate primers (Table 2) and cloned in pMBLT vector (Dominion-mbl). The resulting plasmids were cut with the appropriate restriction enzymes and cloned in the corresponding sites of pCHESI Ω Km polylinker. The resulting plasmids were mobilized into *T. aromatica* strain AR-1 by triparental mating (see below), and Km^r recombinant clones were selected. The nature of the mutation in selected kanamycin-resistant clones was confirmed by PCR using a pCHESI Ω Km-based primer and a second primer located in the region flanking the cloned truncated fragment, as described previously (12). A clone of each mutant was selected, and the correct insertion of pCHESI Ω Km was confirmed by Southern blotting. Mutant strains with inactivated chromosomal versions of *korAB*, *btdL*, and *qorA* were generated by double homologous recombination using plasmid pKNG101 as described previously (13). In short, the gene of interest flanked by 0.5- to 1-kb neighboring regions was amplified with suitable primers (Table 2), cloned in pMBLT, and then inactivated by insertion of the gentamicin resistance cassette from pBBR-MCS5 (14) (for *korAB* and *qorA*) or the kanamycin resistance gene from pACYC177 (15). The resulting mutated region was cloned in the suicide plasmid pKNG101 and was mobilized into *T. aromatica* strain AR-1 by conjugation (see below). Transconjugants selected as gentamicin resistant and streptomycin-sensitive clones were confirmed by PCR and Southern blotting. The use of sucrose for the selection of double recombinants was not efficient in

T. aromatica strain AR1 and was skipped in our screening protocol. The *bqdL qorA* double mutant was obtained in the same way, except that the pKNG101 derivative containing the kanamycin-interrupted *btdL* gene was transferred to the *T. aromatica qorA* mutant strain.

Plasmid construction. For the complementation of the mutant strains, derivatives of broad-host-range plasmid pJB3Tc19 (16) harboring the gene of interest were constructed as follows. The DNA region encompassing the gene(s) of interest was amplified by PCR in a total volume of 50 μ l containing 150 ng chromosomal DNA, 2.6 U Expand high-fidelity DNA polymerase (Roche, Mannheim, Germany), a 300 nM concentration of the appropriate oligonucleotides (Table 2), 3% (vol/vol) dimethyl sulfoxide (DMSO), 300 nM deoxynucleoside triphosphates (dNTPs), and 1 \times Expand high-fidelity buffer with 1.5 mM MgCl₂. The PCR products were purified with the QIAquick gel extraction kit (Qiagen) and cloned in pGEMT Easy (Promega). The resulting plasmids were sequenced to rule out the presence of possible mutations and digested with HindIII/XbaI, and the fragment harboring the amplified gene(s) was ligated with the pJB3Tc19 vector digested with the same enzymes. The resulting constructs bearing the different pathway genes under the control of the P_{lac} promoter were transferred to *T. aromatica* strain AR1 through triparental conjugation.

Triparental conjugation. Mutations were transferred to *T. aromatica* strain AR-1 chromosome by RP4-mediated mobilization. *T. aromatica* strain AR-1 was grown to saturation in Widdel minimal medium supplemented with succinate (5 mM). The *E. coli* donor strain CC118 λ pir bearing the corresponding mutagenic pCHESI Ω Km or pKNG101 derivatives and the *E. coli* HB101 (pRK600) helper strain were grown overnight on LB medium in the presence of kanamycin or chloramphenicol, respectively. All steps were performed aerobically as follows. One milliliter of *E. coli* cultures and 15 ml of the *T. aromatica* strain AR-1 culture were harvested by centrifugation (13,000 \times g for 10 min at 10°C). Cell pellets were washed once with 1 ml of Widdel minimal medium. The three resulting cell pellets were combined in 100 μ l minimal medium, distributed on a sterile 47-mm-diameter, 0.22- μ m-pore-size filter (Schleicher and Schuell, Germany) placed on an LB plate, and incubated overnight at 30°C. The filters were transferred into 1 ml of minimal medium, and cells were washed off by vigorous vortexing. *T. aromatica* strain AR-1 transconjugants were selected by their resistance to kanamycin (pCHESI Ω Km mutants) or gentamicin (double homologous recombination mutants obtained with pKNG101 derivatives) either anaerobically in Widdel minimal medium supplemented with succinate (5 mM) or aerobically in Widdel minimal medium supplemented with glutarate (5 mM) to counterselect against *E. coli* donor and helper strains. The correct insertion of the mutations was confirmed by PCR analysis and Southern blotting. Complementation plasmids were transferred to *T. aromatica* AR-1 mutant strains by RP4-mediated mobilization as described above, except that *T. aromatica* AR-1 mutant transconjugants were selected aerobically by their resistance to tetracycline in Widdel minimal medium supplemented with glutarate (5 mM).

RNA preparation. *Thauera aromatica* strain AR-1 was grown at 30°C under nitrate-reducing conditions using 2 mM α -resorcyate, 5 mM succinate, or both compounds as carbon sources. Cells (45 ml) were harvested by centrifugation (8,000 \times g, 5 min, 4°C) in disposable plastic tubes precooled in liquid nitrogen, and the pellets were kept at -80°C until use. RNA was extracted using the TRI reagent method (Ambion, Austin, TX) with the following modifications: the lysis step was carried out at 60°C, and a final digestion step with RNase-free DNase was added at the end of the process. The RNA concentration was determined with a NanoDrop instrument (Thermo Scientific), and RNA integrity was assessed by agarose gel electrophoresis.

RT-PCR assays. Reverse transcriptase PCR (RT-PCR) was done with 400 ng RNA in a final volume of 50 μ l using the Titan OneTube RT-PCR system according to the manufacturer's instructions (Roche Laboratories). cDNA was synthesized with random primers at 50°C for 45 min, and the PCR cycling conditions were as follows: 94°C for 20 s, 35 cycles at an

adequate annealing temperature for 20 s, and extension at 68°C for 20 s. The annealing temperature was calculated for each reaction based on the melting temperatures of the pair of primers used. Positive (*T. aromatica* strain AR-1 DNA) and negative (total RNA of the *T. aromatica* wild type and mutant strains without reverse transcriptase) controls were included in all assays. The primers used to test cotranscription are listed in Table 2.

Preparation of cell extracts. All steps in the preparation of cell extracts were performed under anoxic conditions. Cultures of *T. aromatica* strain AR-1 and its knockout mutants were grown in 500-ml infusion bottles with a mixture of 1 mM 3,5-DHB and 2 mM succinate as the carbon source. Cells were harvested and washed once with 100 ml of 50 mM potassium phosphate buffer (pH 7.0). Unless used immediately, cell pellets were frozen in liquid nitrogen and stored at -20°C. To prepare cell extracts, cells were suspended in 50 mM potassium phosphate buffer (pH 7) and passed through a French press at 100 MPa. The crude extract was separated from cell debris by centrifugation at 27,000 \times g for 20 min at 4°C. Protein content was quantified with the Bradford method (17).

Determination of 3,5-DHB hydroxylase activity. All measurements of enzyme activities were performed under anoxic conditions at 30°C in 5-ml Hungate tubes or in 1.5-ml cuvettes using anoxic buffers and solutions. Tubes and cuvettes were flushed with nitrogen gas and closed with butyl septa. All additions and samplings were performed with gas-tight Unimatrix microliter syringes (Macherey-Nagel, Düren, Germany). Linear correlations of protein amount and reaction rates were checked for all assays. The 3,5-DHB-oxidizing activity, which catalyzes the hydroxylation of 3,5-DHB to 2,3,5-trihydroxybenzoate and is located in the membrane fraction (9), was measured with K₃Fe(CN)₆ as an electron acceptor in a photometric assay following the reduction of K₃Fe(CN)₆ at 420 nm. The assay mixture contained 50 mM Tris-HCl (pH 8.0), cell extract (1 mg protein), and 1 mM K₃Fe(CN)₆, and the reaction was started by the addition of 1 mM 3,5-DHB. The rate of 3,5-DHB oxidation was calculated from the K₃Fe(CN)₆ reduction rate based on a 2:1 stoichiometry of electron acceptor to electron donor. One unit of 3,5-DHB hydroxylase activity is defined as the amount of enzyme required to convert 1 μ mol of 3,5-DHB in 1 min.

Analytical determinations. To detect the presence of hydroxyhydroquinone in the cultures, culture samples (1 to 4 μ l) were dried under a nitrogen flow to evaporate water, and the dried pellet was directly resuspended in 50 μ l of the derivatizing agent *N,O*-bis(trimethylsilyl)trifluoroacetamide (BSTFA)-trimethylchlorosilane (TMCS) (99:1). The resulting samples were analyzed by gas chromatography-mass spectrometry (GC-MS) in a Varian GC-240MS gas chromatograph coupled with a Varian 240 MS ion trap mass spectrometer. The system was equipped with electronic flow control, a 1079 universal capillary injector, and a CTC CombiPal autosampler. Analytes were separated on a SLB-5ms column (30 m by 0.25 mm by 0.25 μ m) (Supelco, Sigma-Aldrich). The flow rate was 1 ml/min using He as the carrier gas. The column temperature was held at 50°C for 5 min and then increased at 10°C/min to 300°C, which was held for 5 min. The sample (1 μ l) was injected at a 250°C injector temperature in splitless mode (splitless time, 5 min). The mass spectrometer was operated in electron impact ionization mode, acquiring in full scan (50 to 800 atomic mass units), and SIM mode (recording the most abundant ions). The trap and transfer line temperatures were 240°C and 250°C, respectively. MS Workstation software version 6.9.1 was used for instrument control. Detection of compounds was performed using both the NIST08 database and pure standards for comparison. The presence of other intermediates in the culture medium was detected by high-pressure liquid chromatography (HPLC) with a C₁₈ reverse-phase column (Grom, Herrenberg, Germany) and a UV detector (Beckman). The mobile phase was a 1:1 mixture of 100 mM ammonium acetate (pH 2.6) and methanol at a flow rate of 1 ml/min.

Sequence analysis. Nucleotide and amino acid sequences were analyzed using the tools provided by the NCBI (<http://blast.ncbi.nlm.nih.gov/Blast.cgi>) and the ExpASY molecular biology server (<http://www.expasy.org>). The functional annotation of the new gene clusters was performed

with Blast2GO based on values for either average similarity to a group of proteins or maximum identity to a specific protein (<https://www.blast2go.com/blast2go-pro/download-b2g>) (18). Protein alignments were performed with ClustalW (<http://www.ebi.ac.uk/Tools/msa/clustalw2>), and the resulting alignments were displayed with boxshade (http://www.ch.embnet.org/software/BOX_form.html). Computational models of the protein three-dimensional structure were built with the Phyre2 Server (<http://www.sbg.bio.ic.ac.uk/phyre2/>) (19). The following servers and database were used to analyze some of the protein sequences: DAS transmembrane prediction server (<http://www.sbc.su.se/~miklos/DAS/>) (20), MEROPS peptidase database (<http://merops.sanger.ac.uk>) (21), and ESTHER esterase and α/β hydrolase enzyme database (<http://bioweb.enscm.inra.fr/ESTHER/general?what=index>) (22).

Correction of *A. anaerobius* annotation. The gene nomenclature of the previously described *A. anaerobius* resorcinol degradation cluster (accession number EF078692) (7) has been modified to comply with standard genetic nomenclature, as follows: *rhLS*, *bqdhLMS*, and *btdhLS* have been changed to *rehLS*, *bqdLMS*, and *btdLS*, respectively. Moreover, the *rehL* start codon has been relocated 366 nucleotides upstream from the initially proposed nucleotide based on its homology to *dbhL*, so that the protein is now 122 residues longer (see Fig. S1a in the supplemental material); a new gene, coding for a cupin family protein, was annotated as *orf12b* between *btdS* and *orf13*. The first 8 nucleotides of the *orf12b* 5' end overlapped with *orf13* 3' end.

Nucleotide sequence accession number. The *T. aromatica* strain AR-1 3,5-DHB-degradation cluster sequence identified in this work has been deposited in GenBank under accession number KJ995609.

RESULTS

Identification of the gene cluster responsible for the anaerobic catabolism of 3,5-DHB in *Thauera aromatica* strain AR-1. *T. aromatica* strain AR-1 and *A. anaerobius* share an oxygen-independent hydroxylation reaction as the initial step for the degradation of 3,5-DHB and resorcinol, respectively (Fig. 1). We expected genes homologous to those of the *A. anaerobius* resorcinol degradation pathway to be present in the *T. aromatica* strain AR-1 chromosome. To verify this hypothesis, we performed a Southern blot of *T. aromatica* strain AR-1 chromosomal DNA cut with different restriction enzymes and hybridized it under nonstringent conditions with probes against *A. anaerobius* pathway genes *rehL*, coding for the resorcinol hydroxylase large subunit, and *bqdl*, coding for the hydroxybenzoquinone dehydrogenase large subunit, which are the first- and the third-step enzymes in the resorcinol degradation pathway, respectively (Fig. 1) (7). Both probes gave hybridization bands with *A. anaerobius* and *T. aromatica* strain AR-1 DNAs, while no signal was observed with *Pseudomonas putida* KT2440 DNA, used as a negative control (see Fig. S1 in the supplemental material). To map the *T. aromatica* strain AR-1 gene cluster for the 3,5-DHB degradation pathway, we constructed a cosmid library of the *T. aromatica* strain AR-1 chromosome. Several cosmids were selected after colony hybridization with different *A. anaerobius* probes and were sequenced to finally assemble a 36,128-bp fragment showing homology with the *A. anaerobius* resorcinol degradation cluster (see Materials and Methods). Analysis of this sequence defined 28 open reading frames (ORFs), three of which (*orf8*, *orf9*, and *orf24*) used the alternative start codon GUG. In all of them except *orf1*, *orf3*, *orf7*, and *orf19*, a conserved Shine-Dalgarno sequence (consensus, AGGAGG) could be identified at 4 to 10 nucleotides upstream from the start codon. The ORFs were compared with sequences in the databases. As expected, several ORFs showed a high degree of identity to genes of

the *A. anaerobius* resorcinol degradation pathway (Fig. 2 and Table 3; see Table S1 in the supplemental material).

Genes of the first pathway enzyme, 3,5-DHB hydroxylase.

The products of *orf7* and *orf8* showed 60 and 53% identity to the α and β subunits of the *A. anaerobius* resorcinol hydroxylase, respectively, suggesting that these genes coded for 3,5-DHB hydroxylase. The genes were annotated as *dbhL* and *dbhS*. We constructed site-directed insertion mutants of the different genes in the *T. aromatica* chromosome, using either single or double recombination (see Materials and Methods). *dbhL* and *dbhS* knockout mutants were unable to grow with 3,5-DHB as a carbon source, confirming the crucial role of these genes in 3,5-DHB degradation (Fig. 3A). Both mutants could be complemented by a broad-host-range plasmid bearing the two genes under the control of the P_{lac} promoter, ruling out possible polar effects on downstream genes. However, growth both on succinate (data not shown) and on 3,5-DHB was significantly delayed, which we attributed to inefficient growth in the presence of two antibiotics (Fig. 3B). Resorcinol hydroxylase activity was determined in cell extracts of wild-type, *dbhL* mutant, and *dbhS* mutant *T. aromatica* cells grown with 2 mM succinate in the presence of 1 mM 3,5-DHB to induce the pathway. Figure 4 shows that 3,5-DHB hydroxylase was impaired in both mutants, although the *dbhS* mutant reached low activity levels after 72 h, suggesting that a different protein could substitute for this electron transfer protein with low efficiency.

We could identify a molybdopterin-binding domain in the *DbhL* sequence, which classified this protein in the MopB superfamily of molybdopterin-binding proteins (see Fig. S2a in the supplemental material). Proteins known to bind a molybdopterin cofactor generally require a dedicated chaperone to bind the molybdenum-charged cofactor and further direct the protein to the membrane (23) (see below).

Two genes are required for efficient hydroxyhydroquinone oxidation. The product of the 3,5-DHB hydroxylase reaction is the unstable intermediate 2,3,5-trihydroxybenzoate, which is further transformed to hydroxyhydroquinone in the cytoplasm (9) (Fig. 1). The enzyme responsible for this reaction has not been identified, although spontaneous decarboxylation of 2,3,5-trihydroxybenzoate has also been suggested (9). Hydroxyhydroquinone is then oxidized to hydroxybenzoquinone, a reaction mediated by hydroxyhydroquinone dehydrogenase, which has been detected in the membrane fraction of 3,5-DHB-grown *T. aromatica* strain AR-1 cells (10). The gene product of *orf11* in the *T. aromatica* cluster showed 35% identity to the *A. anaerobius* large subunit of hydroxyhydroquinone dehydrogenase, encoded by the *btdL* gene. We annotated *orf11* as *btdL*. Growth of a *btdL* mutant on 3,5-DHB was significantly affected (Fig. 3A). In addition, an *orf26* mutant showed reduced growth on 3,5-DHB (Fig. 3A) and after 24 h accumulated a pink intermediate that was identified as hydroxyhydroquinone by GC-MS (Fig. 5), suggesting that metabolism of this compound was impaired in the *orf26* mutant. Hydroxyhydroquinone was shown to be highly toxic to *T. aromatica* cells even at low concentrations (D. Pacheco, unpublished data), and accumulation of this intermediate in the *orf26* mutant probably caused growth arrest. The product of *orf26* showed 64% identity to a hypothetical quinone oxidoreductase belonging to the medium-chain reductase/dehydrogenase (MDR) family (24). Oxidoreductases of this type catalyze the conversion of alcohols to aldehydes or ketones, suggesting that the *orf26* gene product

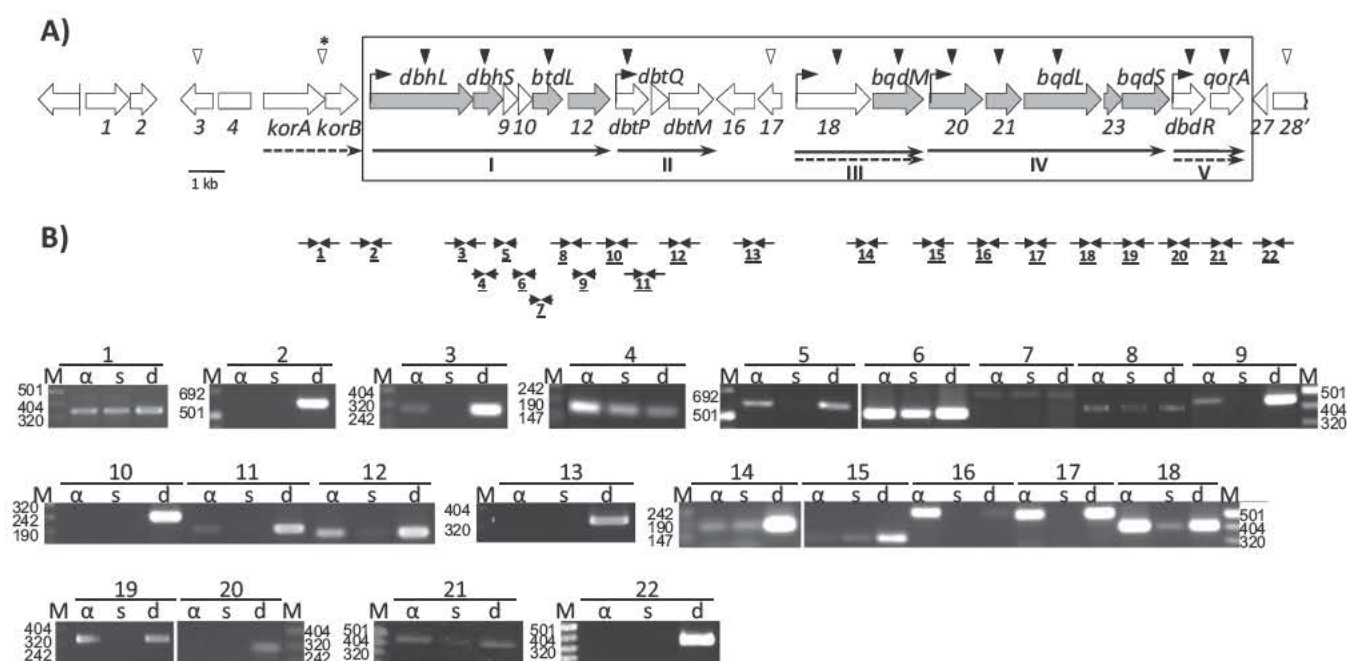


FIG 2 Transcriptional organization of the *T. aromatica* strain AR-1 genomic region coding for anaerobic 3,5-DHB degradation. (A) Genes having a homolog in *A. anaerobius* resorcinol degradation cluster are shaded in gray. A pseudogene with no stop codon (labeled 4) is depicted as a box with no arrowhead. The truncated *orf28* at the end of the cluster is labeled 28'. A triangle above the gene indicates that a knockout mutant with an impaired (black) or wild-type (white) growth phenotype has been obtained. An asterisk indicates a mutant with a deletion encompassing part of *korAB* genes. The operons identified in this work are shown below the genes as solid (inducible) or dashed (constitutive) arrows. Curved arrows above the genes show the presence of putative promoters, as deduced from our results. The group of genes constituting the degradation cluster is boxed. (B) RT-PCR analysis of the 3,5-DHB degradation cluster transcripts. Agarose gels show the RT-PCR products with template RNA isolated from *T. aromatica* strain AR-1 cells grown on succinate (s) or 3,5-DHB (α). The converging black arrows and underlined numbers indicate the amplified region and refer to the PCR products shown below them: M, molecular marker; d, positive control with *T. aromatica* DNA.

would carry out the oxidation of hydroxyhydroquinone to hydroxybenzoquinone. We annotated the *orf26* gene as *qorA*. Thus, efficient processing of hydroxyhydroquinone during 3,5-DHB degradation in *T. aromatica* strain AR-1 required the joint activity of both enzymes. As expected, a *btdL* and *qorA* double mutant was unable to grow on 3,5-DHB (Fig. 3A).

Genes for hydroxybenzoquinone degradation. The products of *orf19*, *orf22*, and *orf24* showed 65, 74, and 53% identity, respectively, with gene products of *A. anaerobius*; these were likely to constitute the third step in the resorcinol degradation pathway and were annotated as *bqdM*, *bqdL*, and *bqdS* (Fig. 2 and Table 3; see Table S1 in the supplemental material). These genes showed a high degree of similarity with the three components of the multi-enzyme complex of pyruvate dehydrogenase. The *bqdL* gene was essential for growth on 3,5-DHB (Fig. 3A). Growth on 3,5-DHB was restored when the pJB-*bqdL* plasmid, harboring the wild-type *bqdL* gene under the control of P_{lac} was introduced into the mutant strain (Fig. 3B). A mutant with a mutation in *bqdM*, encoding the predicted medium-sized component of the enzyme, was also impaired in its capacity to grow on 3,5-DHB, but it still grew on this substrate at a lower rate and reached significant growth values after 1 week (Fig. 3A). This mutant accumulated a colored intermediate in the culture medium; HPLC analysis of the culture supernatant showed two unidentified peaks with retention times of 14.48 min and 10.16 min, which increased with time to reach maximum values when the substrate was completely consumed (not shown).

Genes of unknown function common to the *A. anaerobius* and *T. aromatica* strain AR-1 dihydroxy aromatic degradation pathways. A *T. aromatica* *orf20* mutant was unable to grow on 3,5-DHB (Fig. 3A). This gene was homologous to *A. anaerobius* *orf12* in the resorcinol degradation cluster, which was not essential for growth with resorcinol (7) (see Table S1 in the supplemental material). The product of *orf20* showed a strong similarity with succinate semialdehyde dehydrogenases, enzymes generally involved in the oxidation of aliphatic and aromatic aldehydes. The presence of the homologous *orf12* in *A. anaerobius* suggests that this enzyme could be involved in the last steps of the degradation from HBQ to acetate and malate, as suggested for this strain (7). The *orf20* mutant could be complemented by pJB-*orf20*, harboring the wild-type gene under the control of P_{lac} (Fig. 3B).

The product of *orf21*, which is homologous to *orf10* of the *A. anaerobius* resorcinol degradation cluster (see Table S1 in the supplemental material), belonged to the COG0523 family of "P-loop" GTPases, putative insertases/metallochaperones involved in metallocenter biosynthesis (25), although they were both predicted to function only as insertases, suggesting that they required an accessory metallochaperone. Frequently, insertases are located near metalloproteinases and proteins involved in molybdopterin cofactor recycling. A gene coding for a peptidase was found in both the 3,5-DHB degradation (*orf12*) (Table 3) and *A. anaerobius* resorcinol degradation clusters (7). It is thus tempting to suggest that the products of *orf21* and *orf12* may participate coordinately in the maturation of DbhL. Although *A. anaerobius* *orf10* was not

TABLE 3 Properties of the genes present in the *T. aromatica* AR-1 3,5-DHB degradation cluster and their gene products

Properties		Related gene product										
Gene	Protein accession no.	% GC content	Distance to next gene (bp)	Product size (amino acids/kDa)	pI	Product	% similarity ^a	% identity ^b	E value	Accession no.	Hypothetical function of closest homolog	Organism
<i>orf1</i>	AIO06081	69	8	410/44.8	9.07	9.07	68	74	2e-148	ACK54553.1	Glycyltransferase	<i>Thauera</i> sp. MZ1T
<i>orf2</i>	AIO06100	65	626	260/29.8	7.38	7.38	74	83	5e-110	ACK54554.1	Metallophosphoesterase	<i>Thauera</i> sp. MZ1T
<i>orf3</i>	AIO06082	67	204 ^c	308/33.2	9.59	9.59	53	56	1e-63	EED66667.1	LysR-type transcriptional regulator	<i>Comamonas testosteroni</i>
<i>orf5</i>	AIO06101	70	2	576/60.5	6.38	6.38	69	100	0.0	CAA12243.2	Oxoglutarate-ferredoxin oxidoreductase, α subunit	<i>Thauera aromatica</i>
<i>orf6</i>	AIO06083	70	376	307/32.6	6.70	6.70	79	97	4e-157	CAD27440.1	Oxoglutarate-ferredoxin oxidoreductase, β subunit	<i>Thauera aromatica</i>
<i>dbhL</i>	AIO06084	65		981/110.6	7.02	7.02	60	60	0.0	ABK58620.1	Resorcinol hydroxylase, α subunit	<i>Azoarcus anaerobius</i>
<i>dbhS</i>	AIO06085	65	15	288/32.3	7.10	7.10	58	53	3e-79	ABK58619.1	Resorcinol hydroxylase, β subunit	<i>Azoarcus anaerobius</i>
<i>orf9</i>	AIO06103	62	20	137/15.9	5.65	5.65	50	29	5e-06	EFW04169.1	Mannose-1-phosphate guanylyl transferase	<i>Coprobacillus</i> sp. 29_1
<i>orf10</i>	AIO06086	68	30	114/11.9	6.06	6.06	45	28	0.35	EEP26949.1	Unknown	<i>Abiotrophia defectiva</i>
<i>brdL</i>	AIO06087	74	102	293/29.5	6.0	6.0	63	50	8e-69	ABM15958.1	6-Phosphogluconate dehydrogenase	<i>Mycobacterium vanbaalenii</i>
<i>orf12</i>	AIO06088	67	98	417/46.5	5.50	5.50	68	93	0.0	ABK58632.1	M24 peptidase family	<i>Azoarcus anaerobius</i>
<i>dbtP</i>	AIO06102	68	72	321/35.2	6.99	6.99	53	40	2e-56	CAL95041.1	TRAP transporter, periplasmic protein	<i>Azoarcus</i> sp. BH72
<i>dbtQ</i>	AIO06104	67	4	163/17.8	9.73	9.73	52	34	8e-07	CAL95042.1	TRAP transporter, small permease	<i>Azoarcus</i> sp. BH72
<i>dbtM</i>	AIO06105	64	123	423/44.4	5.21	5.21	64	50	6e-95	CAL95043.1	TRAP transporter, permease	<i>Azoarcus</i> sp. BH72
<i>orf16</i>	AIO06089	66	100	344/37.9	7.77	7.77	66	57	2e-108	ACB33601.1	TRAP transporter, extracytoplasmic receptor	<i>Leptothrix cholodnii</i> sp-6
<i>orf17</i>	AIO06090	74	382	237/25.3	7.68	7.68	65	60	6e-72	EF159106.1	$\alpha\beta$ -Hydrolase	<i>Comamonas testosteroni</i>
<i>orf18</i>	AIO06091	67	64	716/80.0	6.16	6.16	60	53	0.0	CAJ71291.1	Molybdopterin oxidoreductase	" <i>Candidatus</i> Kuenenia stuttgartiensis" ^g
<i>bqdM</i>	AIO06092	69	193	467/49.9	6.26	6.26	80	75	0.0	BAI72155.1	Dihydroliipoamide dehydrogenase	<i>Azospirillum</i> sp. B510
<i>orf20</i>	AIO06093	68	89	499/53.0	5.49	5.49	83	72	0.0	ACD96487.1	Succinic semialdehyde dehydrogenase	<i>Geobacter lovleyi</i> SZ
<i>orf21</i>	AIO06094	70	71	354/38.5	6.21	6.21	59	46	2e-81	ABK58627.1	p47k family protein	<i>Azoarcus anaerobius</i>
<i>bqdL</i>	AIO06095	70	12	735/78.7	5.64	5.64	75	74	0.0	ABK58621.1	Benzoquinone dehydrogenase, α subunit	<i>Azoarcus anaerobius</i>
<i>orf23</i>	AIO06096	68	32	182/20.2	5.95	5.95	72	73	1e-74	ABK58617.1	Glyoxalase	<i>Azoarcus anaerobius</i>
<i>bqdS</i>	AIO06106	72	52	437/44.5	5.98	5.98	65	54	5e-121	CAM75497.1	Pyruvate/ α -ketoglutarate dehydrogenase complex, E2 component	<i>Magnetospirillum gryphiswaldense</i>
<i>dbdR</i>	AIO06107	68	134	317/34.5	7.20	7.20	52	33	1e-36	AAZ63058.1	LysR-type transcriptional regulator	<i>Ralstonia eutropha</i>
<i>qorA</i>	AIO06097	71	232	335/34.9	8.42	8.42	75	68	9e-148	EHP44701.1	Oxidoreductase	<i>Cupriavidus basilensis</i>
<i>orf27</i>	AIO06098	74	233	145/15.9	8.6	8.6	84	79	5e-81	ACK53423.1	Thioredoxin	<i>Thauera</i> sp. MZ1T
<i>orf28^d</i>	AIO06099	72	92				78	83	0	ACK53440.1	(S)-Mandelate dehydrogenase	<i>Thauera</i> sp. MZ1T

^a Average percent similarity to the 20 closest relatives in the databases, as determined with Blast2GO.^b Percent identity with the closest homolog.^c Distance to a pseudogene with no stop codon.^d Data for the available partial sequence.

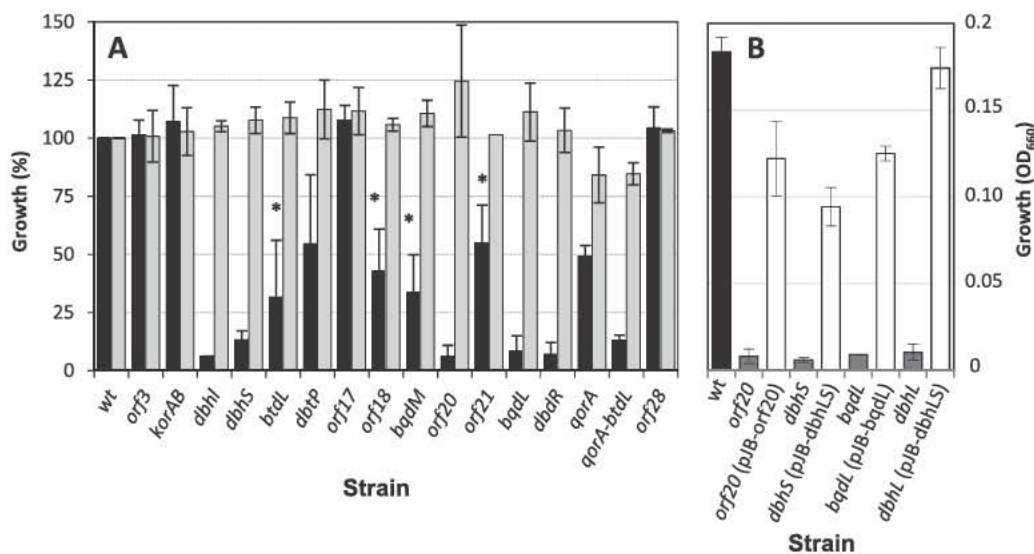


FIG 3 (A) Growth of *T. aromatica* strain AR-1 and the indicated mutants with 5 mM succinate (gray) or 2 mM 3,5-DHB (black) as a carbon source. Growth was determined as OD₆₆₀ after 72 h, except for the *btdL*, *bqdM*, *orf18*, and *orf21* mutants (*), for which growth values were determined after 168 h. Average values from at least 3 repetitions (\pm standard deviation [SD]) are referred to the growth reached by the wild type with each substrate. OD₆₆₀ values for the wild-type strain grown on succinate and 3,5-DHB after 72 h were 0.456 (\pm 0.036) and 0.175 (\pm 0.045), respectively. (B) Complementation of mutant strains with the corresponding wild-type gene. *T. aromatica* strain AR-1 (black), its mutant derivatives (gray), and their complemented strains with pJB3Tc bearing the corresponding wild-type gene (white) were cultivated on 3,5-DHB (2 mM) at 30°C. Growth was determined as OD₆₆₀ after 192 h, except for the *dbhL* mutant and the mutant complemented with pJB:dbhLS, which was determined after 240 h. Average values from at least 3 repetitions (\pm SD) are shown.

essential for growth on resorcinol (7), the growth of a *T. aromatica* *orf21* mutant was significantly delayed (Fig. 3A), although a polar effect on the downstream essential gene *bqdl* could not be ruled out.

Genes unique to the *T. aromatica* strain AR-1 pathway. The remaining genes in the cluster had no counterpart in the *A. anaerobius* resorcinol degradation cluster, but some of them could be annotated with a high degree of confidence. A set of tripartite ATP-independent periplasmic (TRAP) transporter components (*orf13*, *orf14*, and *orf15*) and an additional copy of the extracyto-

plasmic solute receptor (ESR) part of the transporter (*orf16*) could be identified in the middle of the cluster. In addition, a pseudo-gene (*orf4*) with no identified stop codon between *orf3* and *orf5* showed a high degree of similarity with the TRAP transporter ESR. In the products of *orf14* and *orf15*, 4 and 12 transmembrane helices could be predicted, respectively, as expected for integral membrane proteins. TRAP transporter systems have been related to the uptake of carboxylic acids (26), consistent with a role of this set of proteins in 3,5-DHB transport. A mutant with a knockout mutation in *orf13*, encoding the periplasmic component of the TRAP transporter, showed slower growth with 3,5-DHB than the wild type, although it finally reached similar cell densities (see Fig. S3 in the supplemental material). This suggested that this transporter system was required for efficient 3,5-DHB uptake into the cell. Furthermore, transcription analysis showed that *orf13*, *orf14*, and *orf15* constituted an operon that was inducible by 3,5-DHB (see below), supporting the role of this transporter in 3,5-DHB utilization. The three genes were annotated as *dbtP*, *dbtQ*, and *dbtM*, respectively. The 3,5-DHB concentrations found in nature are expected to be much lower than those used in this analysis; thus, utilization of this substrate would probably require the contribution of a dedicated transport system.

Two genes coding for proteins with 100% and 97% identity to the α and β subunits of 2-oxoglutarate-ferredoxin oxidoreductase of *T. aromatica*, which is involved in the regeneration of reduced ferredoxin for benzoyl-CoA reductase (27) (*orf5* and *orf6*, annotated as *korAB*), were located upstream from *dbhL*. The two genes were expressed as one operon and were not induced in the presence of 3,5-DHB (see below). Furthermore, a double mutant in which a region encompassing parts of both genes had been replaced with a gentamicin cassette was unaltered in its capacity to grow with 3,5-DHB as a carbon source, indicating that this electron recycling system was not essential in the pathway (Fig. 3A).

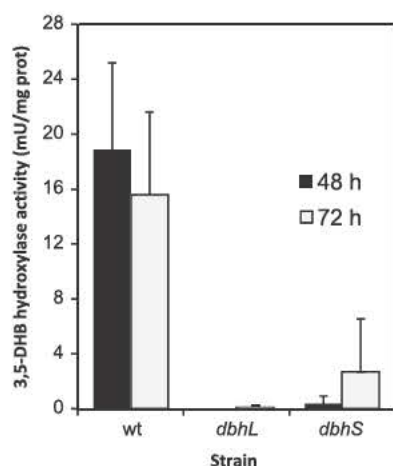


FIG 4 Specific activity of 3,5-DHB hydroxylase in crude extracts of wild-type and mutant *T. aromatica* strain AR-1 cells. Extracts from cells grown for 48 h (black) and 72 h (white) on Widdel medium supplemented with 3,5-DHB (1 mM) plus succinate (2 mM) were obtained as indicated in Materials and Methods. Activity was determined as the rate of 3,5-DHB-dependent $K_3F(CN)_6$ reduction in extracts containing 1 mg of protein.

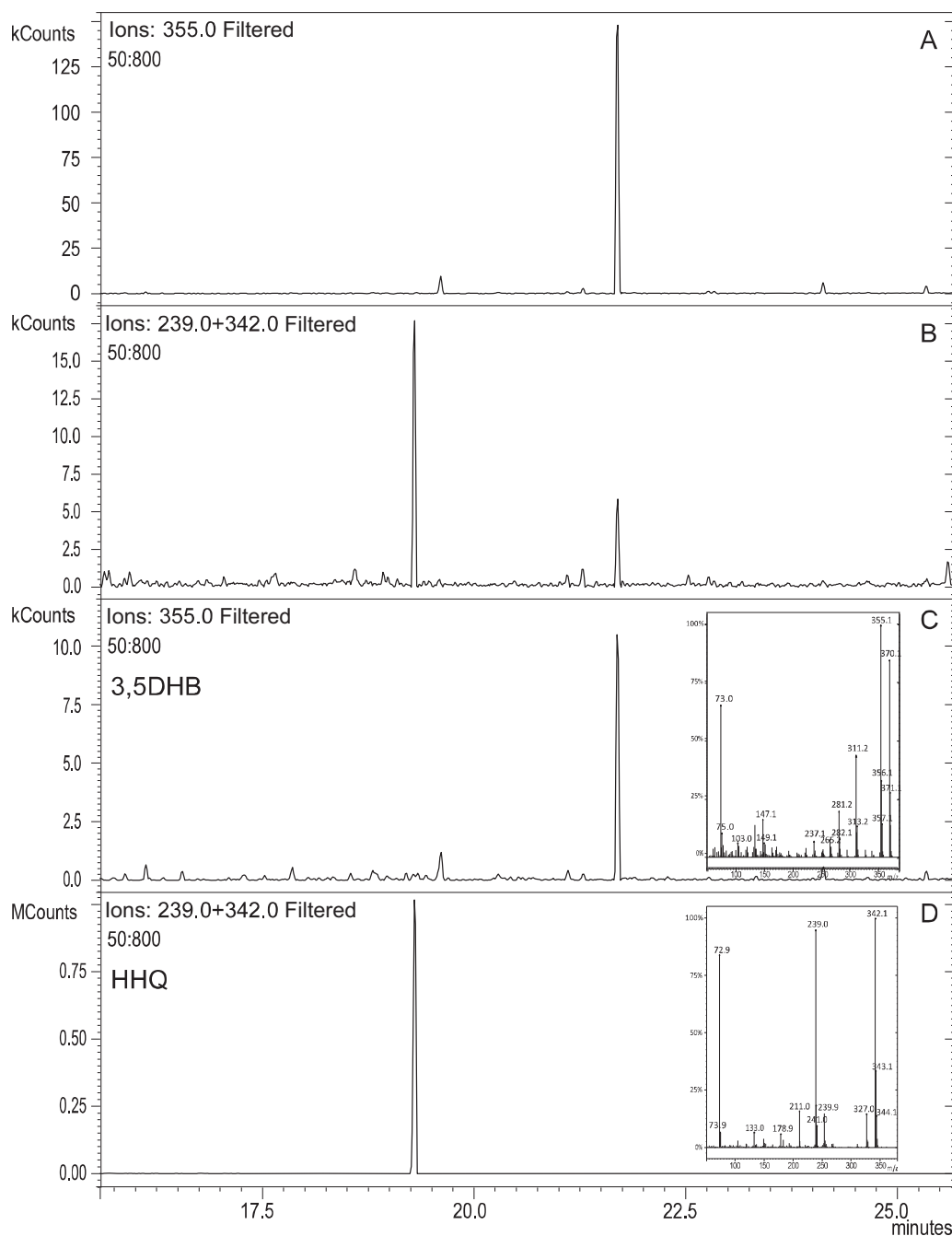


FIG 5 (A and B) GC-MS analysis of the culture supernatant of a *T. aromatica* strain AR-1 *qorA* mutant grown for 72 h on Widdel medium supplemented with 3,5-DHB as a carbon source. (C and D). The GC-MS elution profiles of 3,5-DHB (C) and hydroxyhydroquinone (D) standards are shown for comparison. The mass spectrum of the corresponding trimethylsilyl derivative is included for each standard compound.

An *orf17* insertion mutant was able to grow with 3,5-DHB similarly to the wild type (Fig. 3A). No specific function could be attributed to this gene product, which showed a 65% average similarity with C-C bond hydrolases. The gene product of *orf18* showed homology with molybdopterin oxidoreductases, and in fact it was 39% identical to the *dbhL* (*orf7*) product, although it was 286 residues shorter and was predicted to include a $[\text{Fe}_4\text{-S}_4]$ iron-sulfur center not found in DbhL. An *orf18* mutant was able to grow on 3,5-DHB, although at a lower rate than the wild type

(Fig. 3A). However, a polar effect on the downstream *bqdM* gene could not be ruled out.

Finally, two genes were identified downstream of *qorA*: the product of *orf27*, which was transcribed convergently to *qorA*, showed 79% identity to a *Thauera* MZ1T thioredoxin-like gene possibly involved in mandelate metabolism, and the 5' end of *orf28* allowed the prediction of a protein sequence with 81% identity to a *Thauera* MZ1T gene annotated as mandelate dehydrogenase. An *orf28* knockout mutant was able to grow on 3,5-DHB like

the wild type, suggesting that these two genes with high similarity to the *Thaueria* MZ1T chromosome were unrelated to the 3,5-DHB degradation pathway and constituted the boundary of the cluster in the *T. aromatica* strain AR-1 chromosome (Fig. 3A).

Transcriptional organization and induction of the 3,5-DHB degradation gene cluster. The gene direction and the intergenic distances in the cluster suggested a gene arrangement of at least three operons. To determine the organization of the transcriptional units, we analyzed the cotranscription of each pair of neighbor genes using RT-PCR. It was previously shown that 3,5-DHB degradation enzymes were detected only if the cells were grown with 3,5-DHB as a carbon source, suggesting a substrate-controlled expression of the pathway genes (10). We therefore isolated total RNA from *T. aromatica* strain AR-1 cells growing anaerobically either on succinate or on 3,5-DHB as a carbon source, and we performed RT-PCRs with a series of oligonucleotide pairs covering the different intergenic regions (Fig. 2B). The results defined three transcriptional units that were induced in the presence of the substrate: operon I spanned from *dbhL* to *orf12*, operon II included the three TRAP transporter genes, and operon IV spanned from *orf20* to *bqdB* (Fig. 2). The results also indicated low basal expression levels of a possible internal segment of operon I. In addition, operon III, which covered *orf18* and *bqdB*, and operon V, which included *orf25* and *qorA*, showed basal expression levels during growth on succinate, which seemed to increase in the presence of 3,5-DHB. Semiquantitative RT-PCR assays using increasing RNA concentrations to compare expression levels under induced and uninduced conditions showed amplification of the operon III region at lower RNA concentrations when RNA originated from cells grown in the presence of 3,5-DHB, thus confirming induction of the operon by this substrate (not shown). Finally, the *korAB* genes constituted an independent operon that was expressed independently of the presence of the aromatic substrate, supporting the suggestion that they did not participate in 3,5-DHB degradation. From these results, we could suggest the presence of promoters initiating transcription from *dbhL*, *dbtP*, *orf18*, *orf20*, and *dbdR* (Fig. 2B).

Expression of the pathway is controlled by a LysR-type transcriptional regulator (LTTR). Two genes coding for regulators belonging to the LysR family (*orf3* and *orf25*) were found at both ends of the cluster. Mutations in the two genes were obtained through reverse genetics. Figure 3A shows that an *orf3* mutant could grow on 3,5-DHB like the wild type, indicating that the regulator encoded by *orf3* was not an inducer of this pathway. In contrast, an *orf25* mutant was unable to grow on 3,5-DHB, suggesting that the product of this gene was an essential regulator of the pathway (Fig. 3A). The gene was annotated as *dbdR*. To confirm the role of *dbdR* in the pathway regulation, we determined the expression of the main pathway operons in a *dbdR* mutant background. To this end, we isolated total RNA from the wild-type and *dbdR* mutant strains grown on glutarate plus 3,5-DHB. Transcription of operons I, III, and V was determined through RT-PCR of the intergenic regions *dbhL*-*dbhS* (operon I), *dbtQ*-*dbtM* (operon II), and *orf21*-*bqdB* (operon IV). Figure 6 shows that in the wild-type strain, expression of the operons was induced in the presence of 3,5-DHB, while no amplification product was obtained in the *dbdR* mutant strain grown on succinate plus 3,5-DHB. In contrast, expression of the unrelated *korAB* operon was unaffected by the *dbdR* mutation. The expression pattern in an *orf3* mutant background was similar to that in the wild-type in both the pres-

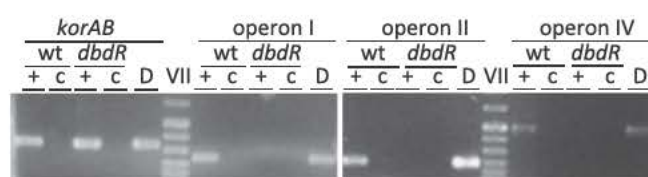


FIG 6 *DbdR* controls expression of the *T. aromatica* strain AR-1 main 3,5-DHB degradation operons. Products of RT-PCR of total RNA from wild-type (wt) and *dbdR* mutant strains of *T. aromatica* strain AR-1 cells grown on 2 mM glutarate plus 2 mM 3,5-DHB (+) are shown. For each operon, a negative control (c) with RNA where the reverse transcription step had been omitted and a positive control with DNA (D) from *T. aromatica* strain AR-1 were included.

ence and absence of 3,5-DHB, ruling out a possible role of the *orf3* product as a repressor of the pathway.

DISCUSSION

A. anaerobius and *T. aromatica* are two betaproteobacteria that share a unique anaerobic degradation pathway for dihydroxylated aromatics that does not proceed through the canonical benzoyl-CoA intermediate; rather, degradation is initiated through oxidation of the aromatic ring, a reaction that is ultimately linked to nitrate respiration. We have shown that the enzymatic similarities between the two strains are reproduced in their genetic complements. Not only were the genes for the three main steps of the pathway conserved, but also homologous auxiliary genes were present in the two clusters (see Table S1 in the supplemental material). A protein pair putatively involved in metalloprotein maturation, conserved in both pathways, could be tentatively annotated: the product of *orf12*, carried in the same operon as *dbhS*, showed 93% identity to the product of the *A. anaerobius* essential gene *orf13*. These proteins were 68% identical to an M24B family peptidase suggested to be involved in protein maturation. The MEROPS database predicted that the product of *orf12* lacked the critical residues required for peptidase activity (21), suggesting that this gene would code for a dedicated chaperone for 3,5-DHB hydroxylase maturation. This was further supported by the presence in the cluster of *orf21*, which coded for a protein showing all sequence features of insertases involved in metalloprotein synthesis and requiring a complementary chaperone (see Fig. S1b in the supplemental material). The presence of the corresponding homologous genes *orf13* and *orf10* in *A. anaerobius* indicates similar processing mechanisms of the enzymatic machinery in both bacteria. Interestingly, two small genes coding for proteins predicted to have a cupin-like structure (*orf9* and *orf10*) were identified in the *T. aromatica* cluster. Cupins are metal-binding proteins involved in a broad diversity of cellular functions (28, 29). We could detect in *A. anaerobius* a previously unidentified ORF between *btD* and *orf13*, which coded for a small protein having a cupin-like structure. The β -barrel structural scaffold defining the cupin fold was clearly predictable for the three gene products (see Fig. S4 in the supplemental material), although like other members of the cupin superfamily, they did not show homology in their amino acid sequences. The presence of these metal-binding protein genes in the clusters was consistent with the presence of several metalloproteins in the two pathways and supports they are involved in similar auxiliary mechanisms. The specific role of each cupin remains to be elucidated.

Generally, folding of proteins such as *DbhL* and *RehL* that bind

Our finding of conserved genetic determinants for dihydroxylated aromatic oxidation in these closely related strains suggests that this degradation strategy was selected in this bacterial group for the efficient degradation of a particular set of aromatic compounds. These pathways with hydroxyhydroquinone as the central intermediate have so far been found only in nitrate-reducing bacteria, which could be explained in terms of the energetic requirements of the reactions involved (5). The oxidation reactions involved in the dearomatization of the two substrates would require electron acceptors of a positive redox potential (the standard redox potentials of the hydroxylating activity are -27 mV for 3,5-DHB, -33 mV for resorcinol, and $+180$ mV for hydroxyhydroquinone dehydrogenation) (6, 9). This does not preclude the presence of additional anaerobic pathways for aromatic degradation channeled through benzoyl-CoA. In fact, a cluster of genes homologous to the *bzd* cluster for benzoate degradation has been found in *A. anaerobius* (J. I. Medina-Bellver, unpublished data), and benzoyl-CoA reductase has been detected by immunoblotting in *T. aromatica* strain AR-1 cells growing on benzoate (10).

ACKNOWLEDGMENTS

This work was supported by FEDER and grants from the Spanish Ministry of Science and Technology (BIO2011-23615), from the Junta de Andalucía (P08-CVI03591), and from the European Union's 7th Framework Program under Grant Agreement no. 312139. Á. Molina-Fuentes was the recipient of an I3P contract from the European Social Funds and a short-term travel grant from the Spanish Ministry of Science and Education to work in Constance. D. Pacheco was the recipient of a Junta de Andalucía predoctoral grant.

We thank Mohamed Khaled-Gijón for excellent technical assistance.

REFERENCES

- Heider J, Fuchs G. 1997. Anaerobic metabolism of aromatic compounds. *Eur J Biochem* 243:577–596. <http://dx.doi.org/10.1111/j.1432-1033.1997.00577.x>.
- Schink B, Philipp B, Müller J. 2000. Anaerobic degradation of phenolic compounds. *Naturwissenschaften* 87:12–23. <http://dx.doi.org/10.1007/s001140050002>.
- Fuchs G, Boll M, Heider J. 2011. Microbial degradation of aromatic compounds—from one strategy to four. *Nat Rev Microbiol* 9:803–816. <http://dx.doi.org/10.1038/nrmicro2652>.
- Boll M, Löffler C, Morris BE, Kung JW. 2014. Anaerobic degradation of homocyclic aromatic compounds via arylcarboxyl-coenzyme A esters: organisms, strategies and key enzymes. *Environ Microbiol* 16:612–627. <http://dx.doi.org/10.1111/1462-2920.12328>.
- Philipp B, Schink B. 2012. Different strategies in anaerobic biodegradation of aromatic compounds: nitrate reducers versus strict anaerobes. *Environ Microbiol Rep* 4:469–478. <http://dx.doi.org/10.1111/j.1758-2229.2011.00304.x>.
- Philipp B, Schink B. 1998. Evidence of two oxidative reaction steps initiating anaerobic degradation of resorcinol (1,3-dihydroxybenzene) by the denitrifying bacterium *Azoarcus anaerobius*. *J Bacteriol* 180:3644–3649.
- Darley PI, Hellstern JA, Medina-Bellver JI, Marqués S, Schink B, Philipp B. 2007. Heterologous expression and identification of the genes involved in anaerobic degradation of 1,3-dihydroxybenzene (resorcinol) in *Azoarcus anaerobius*. *J Bacteriol* 189:3824–3833. <http://dx.doi.org/10.1128/JB.01729-06>.
- Gorny N, Wahl G, Brune A, Schink B. 1992. A strictly anaerobic nitrate-reducing bacterium growing with resorcinol and other aromatic compounds. *Arch Microbiol* 158:48–53. <http://dx.doi.org/10.1007/BF00249065>.
- Gallus C, Schink B. 1998. Anaerobic degradation of α -resorcylylate by *Thauera aromatica* strain AR-1 proceeds via oxidation and decarboxylation to hydroxyhydroquinone. *Arch Microbiol* 169:333–338. <http://dx.doi.org/10.1007/s002030050579>.
- Philipp B, Schink B. 2000. Two distinct pathways for anaerobic degradation of aromatic compounds in the denitrifying bacterium *Thauera aromatica* strain AR-1. *Arch Microbiol* 173:91–96. <http://dx.doi.org/10.1007/s002039900112>.
- Sambrook J, Fritsch EF, Maniatis T. 1989. *Molecular cloning: a laboratory manual*, 2nd ed. Cold Spring Harbor Laboratory, Cold Spring Harbor, NY.
- Llamas MA, Rodríguez-Herva JJ, Hancock RE, Bitter W, Tommassen J, Ramos JL. 2003. Role of *Pseudomonas putida tol-oprL* gene products in uptake of solutes through the cytoplasmic membrane. *J Bacteriol* 185:4707–4716. <http://dx.doi.org/10.1128/JB.185.16.4707-4716.2003>.
- Aranda-Olmedo I, Ramos JL, Marqués S. 2005. Integration of signals through Crc and PtsN in catabolite repression of *Pseudomonas putida* TOL plasmid pWW0. *Appl Environ Microbiol* 71:4191–4198. <http://dx.doi.org/10.1128/AEM.71.8.4191-4198.2005>.
- Kovach ME, Elzer PH, Hill DS, Robertson GT, Farris MA, Roop RM, II, Peterson KM. 1995. Four new derivatives of the broad-host-range cloning vector pBBR1MCS, carrying different antibiotic-resistance cassettes. *Gene* 166:175–176. [http://dx.doi.org/10.1016/0378-1119\(95\)00584-1](http://dx.doi.org/10.1016/0378-1119(95)00584-1).
- Chang AC, Cohen SN. 1978. Construction and characterization of amplifiable multicopy DNA cloning vehicles derived from the P15A cryptic miniplasmid. *J Bacteriol* 134:1141–1156.
- Blatny JM, Brautaset T, Winther Larsen HC, Haugan K, Valla S. 1997. Construction and use of a versatile set of broad-host-range cloning and expression vectors based on the RK2 replicon. *Appl Environ Microbiol* 63:370–379.
- Bradford MM. 1976. A rapid and sensitive method for the quantitation of microgram quantities of protein utilizing the principle of protein-dye binding. *Anal Biochem* 72:248–254. [http://dx.doi.org/10.1016/0003-2697\(76\)90527-3](http://dx.doi.org/10.1016/0003-2697(76)90527-3).
- Conesa A, Götz S, García-Gómez J, Terol J, Talón M, Robles M. 2005. Blast2GO: a universal tool for annotation, visualization and analysis in functional genomics research. *Bioinformatics* 21:3674–3676. <http://dx.doi.org/10.1093/bioinformatics/bti610>.
- Kelley LA, Sternberg MJE. 2009. Protein structure prediction on the Web: a case study using the Phyre server. *Nat Protoc* 4:363–371. <http://dx.doi.org/10.1038/nprot.2009.2>.
- Cserzo M, Wallin E, Simon I, von Heijne G, Elofsson A. 1997. Prediction of transmembrane α -helices in prokaryotic membrane proteins: the dense alignment surface method. *Protein Eng* 10:673–676. <http://dx.doi.org/10.1093/protein/10.6.673>.
- Rawlings ND, Barrett AJ. 1993. Evolutionary families of peptidases. *Biochem J* 290:205–218.
- Hotelier T, Renault L, Cousin X, Negre V, Marchot P, Chatonnet A. 2004. ESTHER, the database of the α / β -hydrolase fold superfamily of proteins. *Nucleic Acids Res* 32:D145–D147. <http://dx.doi.org/10.1093/nar/gkh141>.
- Genest O, Neumann M, Seduk F, Stocklein W, Mejean V, Leimkuhler S, Iobbi-Nivol C. 2008. Dedicated metallochaperone connects apoenzyme and molybdenum cofactor biosynthesis components. *J Biol Chem* 283:21433–21440. <http://dx.doi.org/10.1074/jbc.M802954200>.
- Persson B, Hedlund J, Jornvall H. 2008. Medium- and short-chain dehydrogenase/reductase gene and protein families: the MDR superfamily. *Cell Mol Life Sci* 65:3879–3894. <http://dx.doi.org/10.1007/s00018-008-8587-z>.
- Haas C, Rodionov D, Kropat J, Malasarn D, Merchant S, de Crecy-Lagard V. 2009. A subset of the diverse COG523 family of putative metal chaperones is linked to zinc homeostasis in all kingdoms of life. *BMC Genomics* 10:470. <http://dx.doi.org/10.1186/1471-2164-10-470>.
- Kelly DJ, Thomas GH. 2001. The tripartite ATP-independent periplasmic (TRAP) transporters of bacteria and archaea. *FEMS Microbiol Rev* 25:405–424. <http://dx.doi.org/10.1111/j.1574-6976.2001.tb00584.x>.
- Dörner E, Boll M. 2002. Properties of 2-oxoglutarate:ferredoxin oxidoreductase from *Thauera aromatica* and its role in enzymatic reduction of the aromatic ring. *J Bacteriol* 184:3975–3983. <http://dx.doi.org/10.1128/JB.184.14.3975-3983.2002>.
- Agarwal G, Rajavel M, Gopal B, Srinivasan N. 2009. Structure-based phylogeny as a diagnostic for functional characterization of proteins with a cupin fold. *PLoS One* 4:e5736. <http://dx.doi.org/10.1371/journal.pone.0005736>.
- Dunwell JM, Purvis A, Khuri S. 2004. Cupins: the most functionally diverse protein superfamily? *Phytochemistry* 65:7–17. <http://dx.doi.org/10.1016/j.phytochem.2003.08.016>.
- Ilbert M, Mejean V, Iobbi-Nivol C. 2004. Functional and structural analysis of members of the TorD family, a large chaperone family dedi-

- cated to molybdo-proteins. *Microbiology* 150:935–943. <http://dx.doi.org/10.1099/mic.0.26909-0>.
31. Turner RJ, Papish AL, Sargent F. 2004. Sequence analysis of bacterial redox enzyme maturation proteins (REMPs). *Can J Microbiol* 50:225–238. <http://dx.doi.org/10.1139/w03-117>.
 32. Armstrong RN. 2000. Mechanistic diversity in a metalloenzyme superfamily. *Biochemistry* 39:13625–13632. <http://dx.doi.org/10.1021/bi001814v>.
 33. He P, Moran GR. 2011. Structural and mechanistic comparisons of the metal-binding members of the vicinal oxygen chelate (VOC) superfamily. *J Inorg Biochem* 105:1259–1272. <http://dx.doi.org/10.1016/j.jinorgbio.2011.06.006>.
 34. Thorn JM, Barton JD, Dixon NE, Ollis DL, Edwards KJ. 1995. Crystal structure of *Escherichia coli* QOR quinone oxidoreductase complexed with NADPH. *J Mol Biol* 249:785–799. <http://dx.doi.org/10.1006/jmbi.1995.0337>.
 35. Boyer HW, Roulland-Dussoix D. 1969. A complementation analysis of the restriction and modification of DNA in *Escherichia coli*. *J Mol Biol* 41:459–472. [http://dx.doi.org/10.1016/0022-2836\(69\)90288-5](http://dx.doi.org/10.1016/0022-2836(69)90288-5).
 36. Manoil C, Beckwith J. 1985. TnpA: a transposon probe for protein export signals. *Proc Natl Acad Sci U S A* 82:8129–8133. <http://dx.doi.org/10.1073/pnas.82.23.8129>.
 37. de Lorenzo V, Herrero M, Jakubzik U, Timmis KN. 1990. Mini-Tn5 transposon derivatives for insertion mutagenesis, promoter probing, and chromosomal insertion of cloned DNA in gram-negative eubacteria. *J Bacteriol* 172:6568–6572.
 38. Franklin FC, Bagdasarian M, Bagdasarian MM, Timmis KN. 1981. Molecular and functional analysis of the TOL plasmid pWWO from *Pseudomonas putida* and cloning of genes for the entire regulated aromatic ring meta cleavage pathway. *Proc Natl Acad Sci U S A* 78:7458–7462. <http://dx.doi.org/10.1073/pnas.78.12.7458>.
 39. Gallus C, Gorny N, Ludwig W, Schink B. 1997. Anaerobic degradation of α -resorcylyate by a nitrate-reducing bacterium, *Thauera aromatica* strain AR-1. *Syst Appl Microbiol* 20:540–544. [http://dx.doi.org/10.1016/S0723-2020\(97\)80023-9](http://dx.doi.org/10.1016/S0723-2020(97)80023-9).
 40. Kaniga K, Delor I, Cornelis GR. 1991. A wide-host-range suicide vector for improving reverse genetics in gram-negative bacteria: inactivation of the *blaA* gene of *Yersinia enterocolitica*. *Gene* 109:137–141. [http://dx.doi.org/10.1016/0378-1119\(91\)90599-7](http://dx.doi.org/10.1016/0378-1119(91)90599-7).
 41. Kessler B, de Lorenzo V, Timmis KN. 1992. A general system to integrate *lacZ* fusions into the chromosomes of gram-negative eubacteria: regulation of the Pm promoter of the TOL plasmid studied with all controlling elements in monocopy. *Mol Gen Genet* 233:293–301. <http://dx.doi.org/10.1007/BF00587591>.
 42. Staskawicz B, Dahlbeck D, Keen N, Napoli C. 1987. Molecular characterization of cloned avirulence genes from race 0 and race 1 of *Pseudomonas syringae* pv. *glycinea*. *J Bacteriol* 169:5789–5794.